Evolution of interlayer tunneling spectra and superfluid density with doping in Bi[2]Sr[2]CaCu[2]O[8]+δ

Suzuki, Minoru; Hamatani, Takashi; Anagawa, Kenkichi; Watanabe, Takao

PHYSICAL REVIEW B **85**, 214529 (2012)

Evolution of interlayer tunneling spectra and superfluid density with doping in $Bi_2Sr_2CaCu_2O_{8+\delta}$

Minoru Suzuki,[1,2,*] Takashi Hamatani,[1] Kenkichi Anagawa,[1] and Takao Watanabe[3]
[1]*Department of Electronic Science and Engineering, Kyoto University, Kyoto 615-8510, Japan*
[2]*Photonics and Electronics Science and Engineering Center, Kyoto University, Kyoto 615-8510, Japan*
[3]*Department of Advanced Physics, Hirosaki University, Hirosaki, Aomori 036-8561, Japan*
(Received 15 January 2012; published 26 June 2012)

Interlayer tunneling spectra, the Josephson critical current density J_c, and the normal tunneling resistance have been measured simultaneously for intrinsic Josephson junctions in $Bi_2Sr_2CaCu_2O_{8+\delta}$ over a wide range of doping using a small mesa structure and a short-pulse technique. It is found that J_c decreases by nearly two orders of magnitude in the underdoped region. Experimental J_c is found to show a significant deviation from the theoretical estimates. In order to interpret the result, we propose a model in which the superconducting order parameter is inhomogeneous in **k** space rather than in real space. Based on this model, quasiparticle current-voltage characteristics are calculated, giving a qualitative agreement with the experiment.

DOI: 10.1103/PhysRevB.85.214529 PACS number(s): 74.72.Kf, 74.25.fc, 74.50.+r, 74.78.Fk

I. INTRODUCTION

Although a rich array of experiments has characterized the behavior of high-T_c superconductors (HTSCs), a congruent understanding of high-T_c superconductivity which explains these behaviors has yet to be gained.[1] Recent observation of the quantum oscillation at low temperatures indicates the existence of small electron pockets in the underdoped region,[2,3] while it is also known that holes reside in the Fermi arcs as observed by angle-resolved photoemission spectroscopy (ARPES).[4] As for the pseudogap phenomena,[5] on the other hand, the issue is still unsettled as to whether the pseudogap originates from preformed bosons or from a hidden ordered state. Compared with experiments on the normal-state properties, those on the superconducting properties, and particularly on the superfluid density, are less numerous. It is likely that the superconducting order parameter in HTSCs has the *d*-wave symmetry.[6] As for the superfluid density, it appears that little understanding has been gained since the report of Uemura *et al.*,[7,8] in which the superfluid density increases nearly proportionally to T_c in the underdoped region in HTSCs. This result was, however, deduced based on the averaged distribution of the local magnetic field probed by the muon spin relaxation (μSR) measurement. Therefore, a more direct and sensitive measurement is desired to probe the superfluid density to further understand high-T_c superconductivity. The intrinsic Josephson junction (IJJ) tunneling spectroscopy, as described below, provides a means for such a purpose.

As the Ambegaokar-Baratoff (AB) theory[9] describes, the Josephson critical current density J_c reflects the magnitude of the superconducting order parameter Δ (or the superconducting energy gap Δ_{SG}). Then, simultaneous evaluation of J_c, Δ, and the normal-state tunneling resistance R_N by tunneling spectroscopy can provide a deeper insight into the superfluid density in HTSC. In conventional tunnel Josephson junctions, the interface layers generally tend to degrade. When they are used in tunneling spectroscopy, spectroscopic results reflect the mostly deteriorated interfacial layer rather than the bulk. If we use IJJs,[10,11] however, this is not the case. This is because IJJs are the crystal structure itself and the junction interfaces are clean and flat on an atomic scale, giving rise to ideal tunneling characteristics. The most important point in using IJJs is the fact that the characteristics reflect the bulk properties, since every bit of such a crystal is the IJJ itself. For these reasons, the method using the IJJs is advantageous for the research into the superfluid density through tunneling spectroscopy.

We measured J_c and tunneling spectra almost simultaneously for the IJJs in $Bi_2Sr_2CaCu_2O_{8+\delta}$ (Bi-2212) over a wide range of doping using a very small mesa structure. We found that the coherence peak in the tunneling spectra changes systematically and drastically with doping. Furthermore, we also found that J_c decreases almost exponentially with decreasing doping. These behaviors, which have not been observed in conventional superconductors, are thought to reflect that the superfluid density decreases drastically in the underdoped region. These changes with doping are strongly correlated with the evolution of the pseudogap in this system. In order to interpret the experimental results, we propose a model of an anisotropic superconducting order parameter. We argue that the superconductivity is inhomogeneous in the wave-vector space (**k** space) rather than in real space.

II. EXPERIMENTS

A. Sample fabrication

Samples used in the experiments are small and thin mesa structures consisting of a small number of IJJs in Bi-2212 with various doping levels. The mesa structures were fabricated on a cleaved surface of a Bi-2212 single crystal grown by the traveling-solvent-floating-zone method.[12] First, a 25-nm-thick Ag film was evaporated on a fresh cleaved surface of a crystal. Then, a 50 nm Au film was evaporated. After the evaporation, the crystals were annealed in an infrared image furnace under the conditions described below in an Ar or oxygen atmosphere in order both to improve the contact resistance and to control the doping level at the same time. By adopting the Au/Ag double layer, the contact resistance was reduced significantly after the annealing, while the film surface was kept smooth. The mesa structure was fabricated by standard photolithography and the Ar ion milling technique. After the milling process, a 350-nm-thick SiO film was evaporated and the insulating layer was made by the self-align method. Finally,

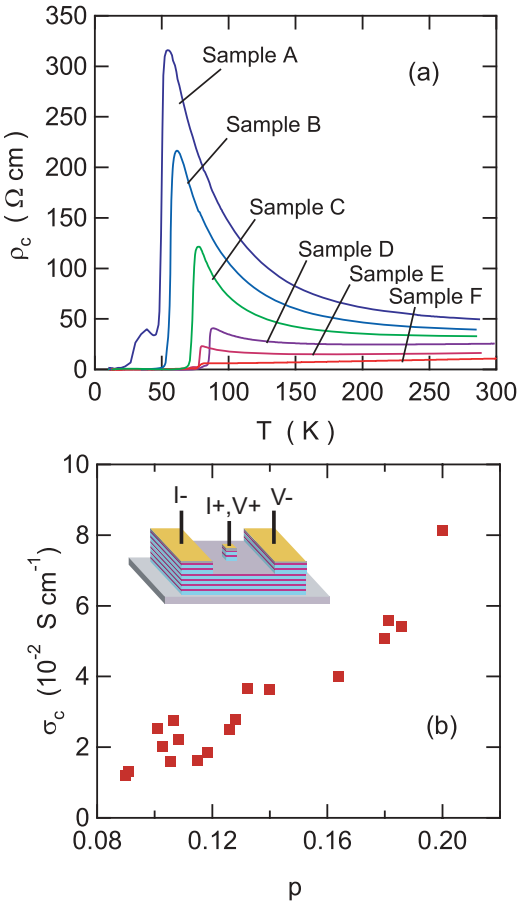

FIG. 1. (Color online) (a) Temperature dependence of ρ_c measured at a bias current of 5 μA for samples A to F in the order of increasing doping. Contact resistances are subtracted for clarity. (b) Plots of σ_c(∼300 K) vs p for various samples including samples A to F. The inset shows a schematic illustration of the mesa structure and the electrode configuration in the present study.

a 450-nm-thick Au film was evaporated and the upper electrode wiring was fabricated by the lift-off method.

The mesa dimensions were 5 to 10 μm on a square side with thicknesses of 7 to 15 nm, which correspond to the IJJ numbers N of 5 ∼ 10. The mesas have electrodes of a three-terminal configuration as illustrated schematically in the inset to Fig. 1(b). The Au/Ag electrode on top of the mesa has a contact resistivity $\rho_{\rm cont}$ (the resistance-area product) of the order of 10^{-6} Ωcm^2. The low contact resistivities were attained by rapid thermal annealing, in which samples were heated to 400∼430 °C at 150 °C/min, then heated to 490∼500 °C in 10 s and held for 10 s, then cooled to 400∼430 °C in 10 s and held for 10∼30 min and then cooled to room temperature at first at 150 °C/min then by the furnace. Underdoped samples were annealed in an Ar atmosphere, while overdoped samples were annealed in an oxygen atmosphere at atmospheric pressure or a little higher. Values for the carrier doping level p, the average number of holes per Cu atom, were determined using the relationship[13] $T_c/T_c^{\rm max} = 1 - 82.6(p - 0.16)^2$ with composition-dependent values for $T_c^{\rm max}$.[14,15] The values for the [Bi]:[Sr] ratio for the Bi-2212 crystals used in the present study and those for $T_c/T_c^{\rm max}$ are shown in Table I.

B. Tunneling measurements

To measure tunneling spectra for IJJs, we employed the short-pulse interlayer tunneling spectroscopy technique,[16–18] in which the data were acquired at a timing of 60 or 160 ns after the pulse peak voltage was reached. The data acquisition was carried out 50 times at a fixed current and the data acquired were averaged. The measurement was carried out twice; first in positive bias and second in negative bias. Values for the current and voltage were measured at a voltage step of 2 to 3 mV per junction, which varied depending on the bias current magnitude. The measured current vs voltage data were smoothed numerically using the least square method. The resolution is no less than 5 mV. The dI/dV-V curves were obtained by numerically differentiating the I-V curves. Other details of the measurements are described elsewhere.[16–19]

In the quasiparticle tunneling measurements, injection of current causes significant Joule heating (i.e., self-heating), even in the short-pulse measurements. It was shown by numerical estimation that the temperature rise is ∼15 K at an injection current corresponding to the superconducting energy gap for a mesa with a similar dimension at a nearly optimum doping.[20] This temperature rise causes an error of approximately 5 to 10% in the magnitude of the superconducting gap. When the samples were in the underdoped region, the current amplitude needed to cover the necessary voltage range was reduced and the self-heating was much less significant. When the samples were in the overdoped region, however, self-heating was significant and the voltage range of the measurements was rather limited.

III. RESULTS

Figure 1(a) shows the temperature T dependence of ρ_c determined from the mesa resistances R_c for various samples from underdoped $p = 0.091$ to overdoped $p = 0.20$ (samples A–F). Figure 1(b) shows plots for the c-axis conductivity $\sigma_c = \rho_c^{-1}$ vs p at ∼300 K, indicating a systematic increase in σ_c with p. T_c of the samples, as determined from the midpoint of the resistive transition, ranges from 50 K for sample A to 86 K for sample D, which is nearly optimally doped. In the figure we subtracted for clarity the contact resistances,[21] which are usually less than 10% of the R_c(300 K) value, or less than ∼30% of R_c(300 K) even in the largest case of underdoped samples. It is clearly seen that the T dependence of ρ_c changes systematically from a metallic behavior to a semiconductor behavior as p decreases, indicating the evolution of the pseudogap. This is because the transport in the c axis in the Bi-2212 system is via tunneling and basically depends on the density of states (DOS) at the chemical potential. Table I lists the sample dimensions and values for ρ_c(300 K), contact resistivity $\rho_{\rm cont}$, and other physical properties for typical samples A to F.

Figure 2 shows the oscilloscope images of the current-voltage characteristics (IVC) at about 10 K for samples A to F. The branch structures in the IVC were used to determine the exact number of IJJs N in the mesas. It is clearly seen that the magnitude of J_c increases as p increases. The magnitude of J_c was determined by averaging the J_c values represented by the I-V branches, except for a few branches whose J_c is

TABLE I. Various physical properties for representative samples A–F: T_c defined at the midpoint of the resistive transition, number of holes at Cu atom p, number of IJJs in a stack N, junction area S, thickness of mesa d, [Bi] : [Sr] ratio of single crystal, ρ_c at 300 K, $2\Delta_{SG}$ at 10 K, $2\Delta_{PG}$ at 10 K and just above T_c, J_c at 10 K, normal tunneling resistance R_N at 10 K, and contact resistivity ρ_{cont} at 300 K. T_c^{max} is 82.7 K for samples A, B, C, E, and 89 K for samples D and F.

Sample	A	B	C	D	E	F
T_c (K)	50.0	60.3	74.9	86.0	78.2	78.0
p	0.091	0.103	0.126	0.140	0.186	0.200
N	9	10	11	9	10	5
S (μm^2)	80.5	61.4	67.7	100	68.2	29.6
d (nm)	13.5	15	16.5	13.5	15	7.5
[Bi] : [Sr]	2.2 : 1.8	2.2 : 1.8	2.2 : 1.8	2.1 : 1.9	2.2 : 1.8	2.1 : 1.9
ρ_c(300 K) (Ω cm)	56.5	39.3	35.8	25.6	16.2	10.8
$2\Delta_{SG}$(10 K) (meV)	82	78	78	72	52	46
$2\Delta_{PG}$(10 K) (meV)	>200	>200	140 ± 11	99 ± 2	86 ± 4	
$2\Delta_{PG}(>T_c)$ (meV)	>200	>200	131 ± 9 (80 K)	112 ± 19 (90 K)	71 ± 11 (80 K)	
J_c (10 K) (kA/cm^2)	0.149	0.228	0.561	1.06	4.69	8.10
R_N (10 K) (Ω)	9.86	9.52	7.30	2.45	2.36	2.43
ρ_{cont} (300 K) ($\mu\Omega$ cm^2)	33.5	15.3	10.1	1.95	2.64	1.14

smaller than the others due to the proximity effect caused by the surface Au/Ag electrode. The J_c values for these samples are listed in Table I.

Figure 3 shows the IVC obtained by the pulse method in an extended V range for samples A to F at various T, representing a systematic change from an almost featureless nonlinear curves for sample A to a large-gap structure for samples D–F. The voltages V are normalized for a single junction. The large subgap resistance in the IVCs at low temperatures indicates that the IJJs are of very high quality and that the characteristics exhibited are nearly ideal. In the V range above the gap voltage, IVCs are nearly linear. It is clearly seen that the slope of the linear IVC changes as the temperature rises. This implies that the self-heating was suppressed sufficiently—in the presence of self-heating, the IVCs coalesce into a single line at higher voltages. It is also noted that the linear IVCs in a higher V range nearly extrapolate to the origin, implying that the self-heating is suppressed. Values for the normal tunneling resistance R_N are obtained from the slope of the IVC at the highest biases for each sample. R_N shows a linear T dependence, probably reflecting the carrier scattering dynamics in the ab plane.[16] The range of the change in R_N is small and the R_N values are roughly equal to R_c at 300 K.[16,22]

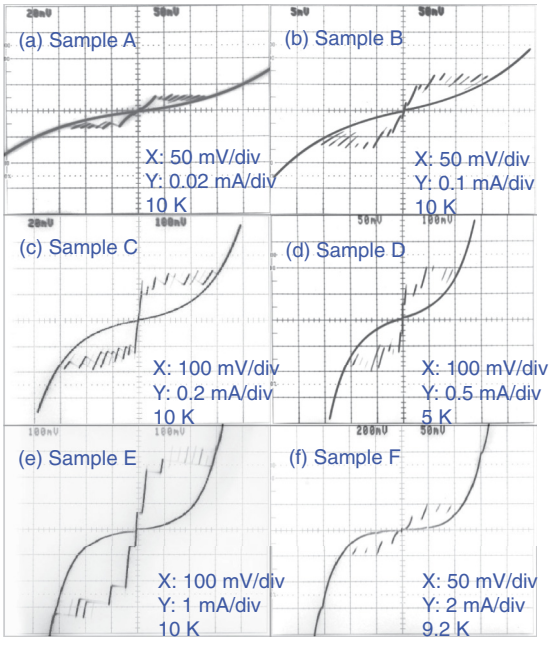

FIG. 2. (Color online) Oscilloscope images for the I-V curves for samples A–F at ~10 K.

The tunneling spectra for samples A to F are shown in Fig. 4 at various temperatures both in the superconducting state and in the normal state. Systematic doping-dependent features are evident in these sets of dI/dV-V curves. First, the most straightforward systematic change is the evolution of the gap structure and the coherence peak at the gap voltage with increasing doping. The sharpness of the superconducting peak for overdoped samples may be partially due to the influence of self-heating, which more or less remains even in the case of small mesa structures and the pulse measurements. In the deeply underdoped sample A, we can see a broad cusp rather than a superconducting peak at the shoulder of the V-shaped background, which barely indicates the existence of superfluid density. From these tunneling spectra, values for $2\Delta_{SG}$ are obtained as half the separation of the superconducting peaks. The magnitude of $2\Delta_{SG}$ shows a tendency to decrease from ~80 meV at $p = 0.09$ to less than 50 meV at $p = 0.20$. This is a tendency observed previously by the intrinsic tunneling spectroscopy as well as by scanning tunneling spectroscopy and others.[23] Another systematic change is seen in the background, which is strongly V shaped in the underdoped region even above T_c and changes with increasing doping to a hump structure accompanied by a dip. This dip and hump structure tends to disappear in the overdoped region, but their traces can be seen in the present results. All these behaviors of the spectra indicate the evolution of the pseudogap, which develops significantly in the underdoped region and is believed to disappear in the overdoped region.

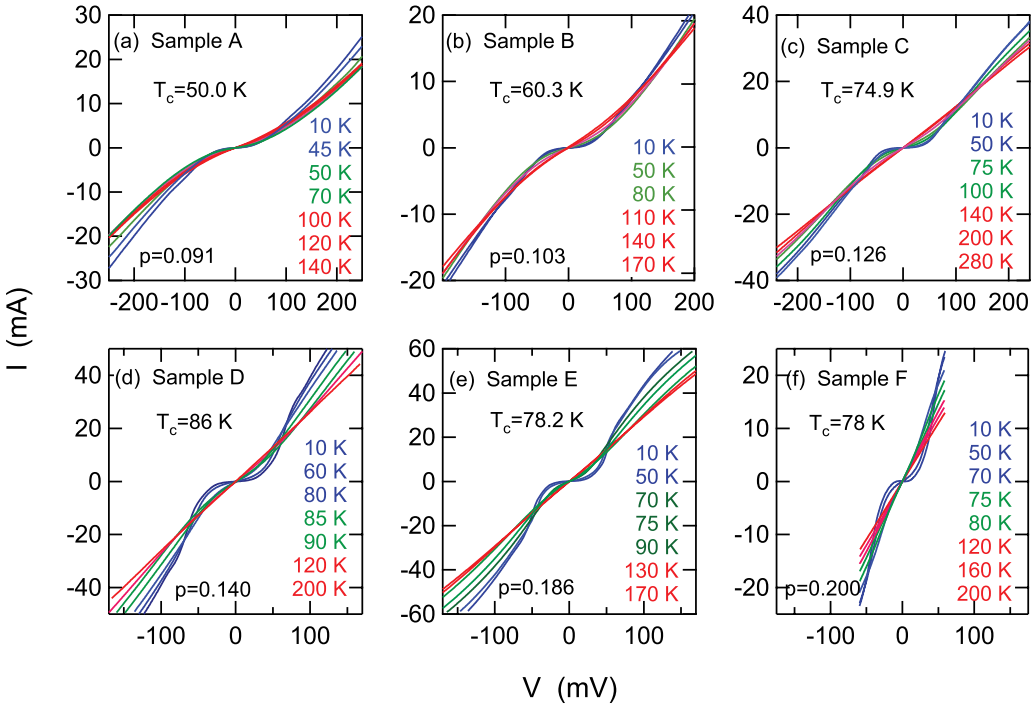

FIG. 3. (Color online) I-V curves measured by the short-pulse method for samples A–F at various temperatures from 10 K to well above T_c.

The pseudogap magnitude $2\Delta_{PG}$ is determined likewise in the case of $2\Delta_{SG}$. It was once reported that the tunneling spectra for the Bi-2212 system can be explained in terms of a single gap with an energy-dependent quasiparticle relaxation time[24] or in terms of a single gap with a temperature-dependent quasiparticle relaxation time.[25,26] However, this is not likely the case in the underdoped region, where the two-gap scenario is likely.[27–29] Typical values for $2\Delta_{SG}$ and $2\Delta_{PG}$ are listed in Table I for samples A to F.

Now, we have various sets of values for J_c, R_N, and $2\Delta_{SG}$ obtained from a single sample for different doping levels. From the values for R_N and $2\Delta_{SG}$, we can obtain a theoretical

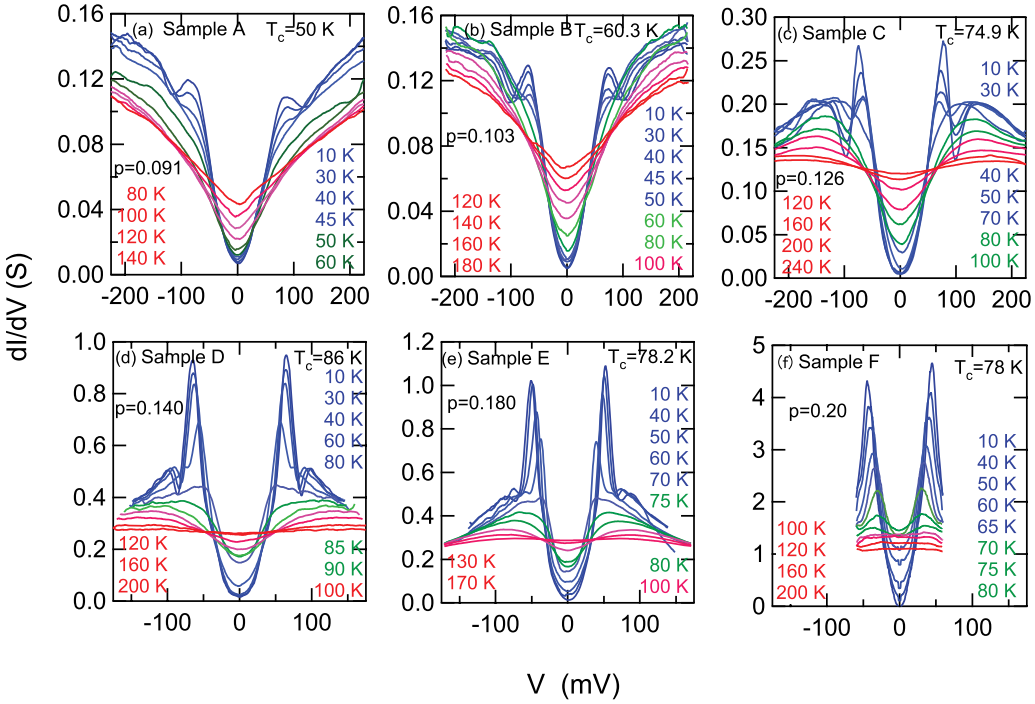

FIG. 4. (Color online) dI/dV-V curves obtained by numerically differentiating the I-V curves measured by the short-pulse method for samples A–F at different temperatures from 10 K to well above T_c.

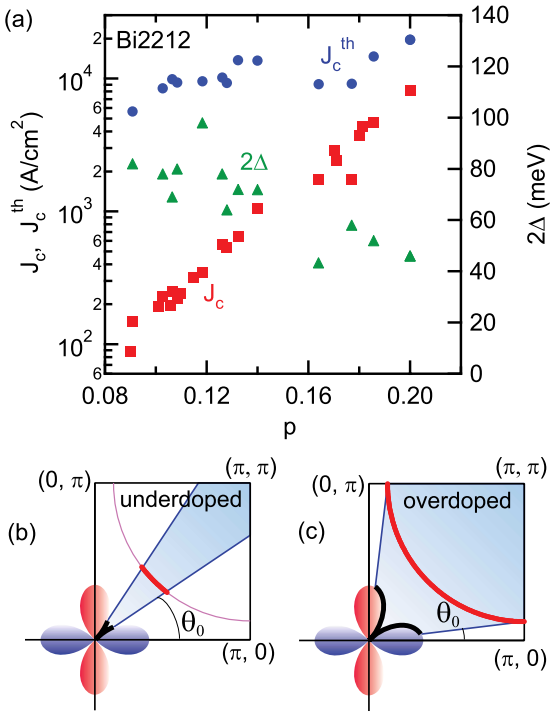

FIG. 5. (Color online) (a) Plots for J_c, J_c^{theor}, and 2Δ as a function of p. (b) Schematic illustration of the relationship between d-wave symmetry lobes and the Fermi arc in the underdoped region, and (c) in the overdoped region. The thick curves on the d-wave symmetry lobes indicate the proportion of the contribution to the superfluid density.

estimate for the critical Josephson current density, J_c^{theor}, which is to be compared with the present experimental results.[9] If there is a discrepancy between the experimental data and the theoretical estimates, it implies to a greater degree that there is a deviation from a homogeneous Josephson junction model. Namely, it implies that the superconducting order parameter is inhomogeneous, because the IJJs reflect the bulk properties. In this regard, one may conjecture a different view, in which imperfections in the barrier layer may cause a deviation from the theory. However, this is unlikely. In the present case, such factors that influence the magnitude of J_c are already included in R_N. Therefore, the present method provides the value of J_c^{theor} that should be equal to the experimental data when Δ is homogeneous, even if the barrier layers contain imperfections. Furthermore, since we have used IJJs in the present study, such imperfections are eliminated to the limit which is supposed for a single crystal. Therefore, a large deviation between the experimental data of J_c and the theoretical estimates of J_c^{theor} implies that an inhomogeneity exists in the superconducting order parameter as a genuine intrinsic bulk property.

The values of experimental J_c are plotted in Fig. 5(a), together with those for $2\Delta_{SG}$, as a function of p for various samples including samples A to F. It is clearly seen that J_c decreases drastically, almost exponentially with decreasing p by nearly two orders of magnitude. Since J_c reflects the magnitude of the superfluid density ρ_s, as described below, it is astonishing that ρ_s decreases by such a large amount despite that the carrier density decreases only moderately. This is the most important result in the present experiment and its cause is the main subject that we address in the remainder of this section and in the following section.

It was reported that charges in the barrier layer in a Josephson junction or those at the periphery of a Josephson junction cause the depression of J_c.[30–33] Since such charges function to change the nearby potential like band bending, the superconducting order parameter is only locally diminished. Furthermore, the range of the change in the potential is of the order of the Thomas-Fermi screening length, which is less than 1 nm in the case of HTSC. Therefore, we can neglect the area of such influences from the charges at the periphery because the junction lateral size is 5 to 10 μm in the present case. This presents a stark contrast with the case of grain boundary Josephson junctions, where the influence of the charges at the periphery or in the barrier layer is significant. Even if such charges are influential, the effect appears as a change in the magnitude of the superconducting order parameter, and it is incorporated into $2\Delta_{SG}$, which is directly measured in the present study. When charges exist in the barrier layer of IJJs, they usually exist in the form of excess oxygen ions in the Bi-O double layers. The excess oxygen ions are thought to provide holes to the CuO_2 double layers. Therefore, it is unlikely that the influence of the charges in the barrier layer in the IJJs causes such a significant decrease in J_c, contrary to the case of grain boundary Josephson junctions.

As an initial step, we compare the experimental results with the theoretical estimates J_c^{theor}. As a theoretical model, we employ the Ambegaokar-Baratoff (AB) theory[9] for an s-wave superconductor. In the AB theory, J_c at low temperatures is represented by

$$J_c^{theor} = \frac{\pi \Delta}{2eR_N S}, \quad (1)$$

where S is the area of the Josephson junction. There may be some concern about the appropriateness of using the s-wave symmetry for the comparison with the experimental results for HTSC, in which the d-wave symmetry has been observed. However, it soon becomes clear that the change in J_c^{theor} arising from the difference between the d-wave and the s-wave symmetries is negligible compared with the difference between the experimental J_c and J_c^{theor}.

Theoretical estimates for J_c^{theor} obtained by using Eq. (1) are plotted in Fig. 5(a) for comparison with the experimental results. It is seen that J_c^{theor} decreases slowly as p decreases. This is a consequence of homogeneous Δ and R_N, both of which vary slowly with p. It is also seen that the theoretical J_c^{theor} is much greater than the experimental J_c, resulting in a significant discrepancy between J_c and J_c^{theor}. Most astonishingly, the discrepancy increases to a value of as large as 10^2 near $p = 0.09$. It should be noticed that this drastic discrepancy between J_c and J_c^{theor} is not due to the change in the tunneling processes such as tunneling probability because such changes are already included in R_N through the estimates of J_c^{theor}, as stated earlier. This is the key point in the present experiment, in which J_c, R_N, and $2\Delta_{SG}$ are obtained from a single IJJ stack simultaneously to remove unknown influence due to tunneling processes. Clearly, the result shown in Fig. 5(a) implies that a model of a homogeneous superconducting order parameter, or a homogeneous superfluid model, fails to explain the experimental J_c. Since the IJJs are almost ideal Josephson

junctions reflecting the bulk superconducting order parameter Δ, the present result implies that Δ in the Bi-2212 high-T_c superconductor is no longer homogeneous.

In the present experiments, we have found two important doping dependencies. First, a significant evolution of the tunneling spectra has been observed: evolution of the superconducting peak with increasing doping, and evolution of the pseudogap with decreasing doping. Second, we have also found that J_c decreases significantly by a factor of two orders of magnitude with decreasing doping level from $p = 0.20$ to 0.09, suggesting a significant variation in the superfluid density with doping. As will be discussed in the following section, the present experimental results imply that both are closely related to each other through the electronic structure of the Bi-2212 system, and determine the superfluid density and the scale of the pseudogap.

IV. DISCUSSION

A. Inhomogeneous Δ in k space

Generally, the magnitude of J_c for a tunnel Josephson junction is reasonably interpreted in terms of the AB theory when Δ and R_N are homogeneous. However, the present experimental result shows that the experimental J_c is orders of magnitude smaller than the theoretical $J_c^{\rm theor}$. At this point, if we notice that the AB theory is based on the constraint that Δ and R_N are homogeneous, it turns out that the present result indicates R_N or Δ or both are no longer homogeneous. Only when they are inhomogeneous is the experimental J_c explicable. Because experimental R_N is used in the theoretical estimates of $J_c^{\rm theor}$, the inhomogeneity must be sought for in Δ. There are two ways in which inhomogeneity modifies Δ. One is inhomogeneity in real space and the other is inhomogeneity in **k** space. For example, d-wave superconductivity is a kind of inhomogeneity in **k** space. However, what we need to invoke is a much more inhomogeneous superconducting order parameter in **k** space.

In order to explain the large discrepancy shown in Fig. 5(a), we need either of the following inhomogeneous superconducting order parameters; namely, a position-dependent $\Delta(\mathbf{r})$ or a wave-vector dependent $\Delta(\mathbf{k})$. In both cases the J_cs are represented by

$$J_c = \frac{\pi}{2eR_N S}\int \Delta(\mathbf{r})\frac{d\mathbf{r}}{S}, \tag{2}$$

or

$$J_c = \frac{\pi}{2eR_N S}\int \Delta(\mathbf{k})\frac{d\mathbf{k}}{S_k} = \frac{a^2}{8\pi eR_N S}\int \Delta(\mathbf{k})\,d\mathbf{k}, \tag{3}$$

where S is the area of the IJJ, and $S_k = (2\pi/a)^2$ is the area of the first Brillouin zone with a being the lattice constant. The former case indicates inhomogeneity in real space, while the latter implies inhomogeneity in **k** space, which we first consider. The d-wave symmetry of $\Delta(\mathbf{k}) = \Delta_0\cos 2\theta$ with $\theta = \tan^{-1}(k_y/k_x)$ in HTSCs is a case of the latter kind. Evidently, however, the d-wave symmetry alone leads to a decrease in J_c by a factor of only $2/\pi$. By no means does this lead to such an almost-extinguishing depression in J_c. Therefore, we need to invoke much stronger and drastic inhomogeneity in **k** space.

In the underdoped region, it was revealed by ARPES that a large Fermi surface is absent and only the Fermi arcs are present in the nodal direction;[4,25,29] that is, in the (π,π) direction, implying that most of the itinerant holes have **k** vectors around the (π,π) direction at low temperatures. On the other hand, the d-wave order parameter has line nodes in the $(\pm\pi, \pm\pi)$ directions in the **k** space. When this is viewed with the d-wave order parameter superimposed on the **k** space, it becomes clear that only a very small proportion of itinerant carriers are used to form superfluid in the underdoped region. The relationship between the Fermi arc and the d-wave order parameter is schematically illustrated in Fig. 5(b). The superfluid density available in this case is drawn by a thick line on the d-wave order parameter, showing that only a small fraction of the superconducting order parameter contributes to the superfluid density. Thus, if the superfluid density in the underdoped region is composed of pairs with a symmetry similar to the d-wave symmetry, it is obvious that the superfluid density becomes rapidly small as the length of the Fermi arc is reduced. When the Fermi arc develops to form a full Fermi surface in the overdoped region, the superfluid density increases significantly, as symbolically represented by the thick lines in Fig. 5(c). This picture (i.e., the **k**-space inhomogeneity), thus explains the significant doping dependence of J_c and the evolving superfluid density with doping. This model is considered as an extreme case of a superconducting order parameter with the magnitude varying as a function of θ.

In the case of d-wave superconductivity, $\Delta(\mathbf{k}) = \Delta_0\cos 2\theta$. Then, Eq. (3) is expressed as

$$\begin{aligned} J_c &= \frac{a^2}{8\pi eR_N S}\iint \Delta_0|\cos 2\theta|\,k\,dk\,d\theta \\ &\simeq \frac{\pi\Delta_0}{2eR_N S}\frac{1}{2\pi}\int_0^{2\pi}|\cos 2\theta|\,d\theta, \end{aligned} \tag{4}$$

where the integral is carried out in the first Brillouin zone. The last equation is obtained by the approximation in which the boundary of the integration is set at a constant of $k = \pi/a$ (i.e., the first Brillouin zone boundary in the k_x direction). Numerical calculation shows that this approximation leads to an error of 2.42%. The integral of Eq. (4) in the case of the pure d-wave symmetry gives a result for J_c, which is a factor of $2/\pi$ smaller than the case of pure s-wave symmetry.

In the case of underdoping, due to the presence of the Fermi arcs, the integral range in Eq. (4) is reduced to $\theta_0 \sim \pi/2 - \theta_0$, where $\pi/2 - 2\theta_0$ indicates the angular range spanned by a single Fermi arc, as depicted in Figs. 5(b) or 5(c). Then we obtain

$$J_c = \frac{\pi\Delta_0}{2eR_N S}\frac{2}{\pi}(1 - \sin 2\theta_0).$$

When θ_0 is close to $4/\pi$, we have an approximate expression, with $\varphi_0 = \pi/4 - \theta_0$,

$$J_c = \frac{2\Delta_0}{eR_N S}\varphi_0^2,$$

indicating that J_c decreases as φ_0^2 when φ_0 is small. Although the result given by this model is only qualitative, it explains sufficiently why J_c decreases very rapidly as the doping level

decreases. Thus, J_c can decrease significantly when the d-wave symmetry of the order parameter is combined with the Fermi arcs (or anisotropic Fermi pockets) even if Δ is homogeneous in real space.

It is also noted that the superconducting order parameter is determined by renormalizing the density of quasiparticles and the superfluid density under a self-consistent condition. A **k**-dependent special distribution of the DOS deriving from the Fermi arcs does not necessarily lead to a pure d-wave symmetry. However, when we take into account the fact that Δ in the optimum doping level is of the d-wave symmetry, it is sufficiently reasonable that the symmetry of Δ in the underdoped region is close to the d-wave symmetry at least in the nodal direction.

In the above model, there are ranges for θ in which the DOS at the chemical potential is absent. In these ranges, extra energy is needed for holes to be itinerant. In other words, the present model implies that, in the underdoped region, the carriers outside the Fermi arcs need extra energy to be itinerant. Then, it is thought that the background structure in Figs. 4(a) and 4(b) is related with such holes, and their distribution is significantly inhomogeneous, reflecting the pseudogap. The energy scale for this excitation is expected to be of the same order of 2Δ and is thought to constitute the pseudogap.[27–29] When the doping is increased, the θ range for the semiconducting transport is reduced and the pseudogap becomes less pronounced. In this sense, the pseudogap is, therefore, a **k**-dependent semiconducting energy gap and is likely to have a symmetry similar to a d wave.[27,34]

B. Quasiparticle I-V characteristics and the pseudogap

In the following, we calculate the quasiparticle I-V characteristics based on the above model, in which $\Delta(\mathbf{k})$ is inhomogeneous in **k** space as depicted in Figs. 5(b) and 5(c). Here, it is sufficient for us to consider the θ range of $0\sim\pi/4$ because of the four-fold symmetry of the d-wave order parameter. For the numerical calculation, it is assumed that the superconducting gap $\Delta(\mathbf{k}) = \Delta_{SG}(\theta)$ spans from θ_0 to $\pi/4$ (the same range spanned by the Fermi arc) and the semiconducting pseudogap $\Delta(\mathbf{k}) = \Delta_{PG}(\theta)$ spans from 0 to θ_0 as expressed by

$$\Delta_{SG}(\theta) = \Delta_0 \cos 2\theta \quad (\theta_0 < \theta < \pi/4), \tag{5}$$

$$\Delta_{PG}(\theta) = r\Delta_0 \cos 2\theta \quad (0 < \theta < \theta_0). \tag{6}$$

For the $\pi/4 < \theta < \pi/2$ region, Δ_{SG} and Δ_{PG} have the symmetric gap structure and the rest are the repetitions. It is assumed that $\Delta_{PG}(\theta)$ has the d-wave symmetry and its magnitude is larger than $\Delta_{SG}(\theta)$ by a factor of r, where r is a parameter. The experimental results indicate that r can be larger than 1.0.[27,35] As for the superconducting region ($\theta_0 < \theta < \pi/4$) the DOS $N_s(E)$ has the form

$$N_s(E,\theta)/N(0) = \mathrm{Re}\frac{E}{\sqrt{E^2 - [\Delta_{SG}(\theta) + i\Gamma]^2}}, \tag{7}$$

where $N(0)$ is the DOS at the chemical potential in the normal state and Γ is the quasiparticle relaxation time placed in the Δ part.[36] For the pseudogap DOS in the $0 < \theta < \theta_0$ region, we simply adopted a smoothed two-dimensional free electron case, as expressed by

$$N_p(E,\theta)/N(0) = \tfrac{1}{2}\tanh[qE - \Delta_{PG}(\theta)] + \tfrac{1}{2}. \tag{8}$$

In addition, it is also assumed that the DOS has an angular dependence similar to the one seen in the two-dimensional tight binding model. In the present case, we use the formalism incorporated by Ozyuzer and coworkers:[37]

$$N(\theta)/N(0) = 1 + \alpha \cos 4\theta, \tag{9}$$

where α is a parameter. Finally, we adopted the coherent tunneling model,[22] where the **k** components in the a-b plane are conserved, by taking into account the special case for the IJJs in which coherent tunneling takes place as it is likewise in a single crystal.

Figures 6(a) and 6(b) show a set of calculated I-V and dI/dV-V characteristics based on the model for parameters indicated in the figures. In the figure, $\beta = \theta/(\pi/4)$ is used as

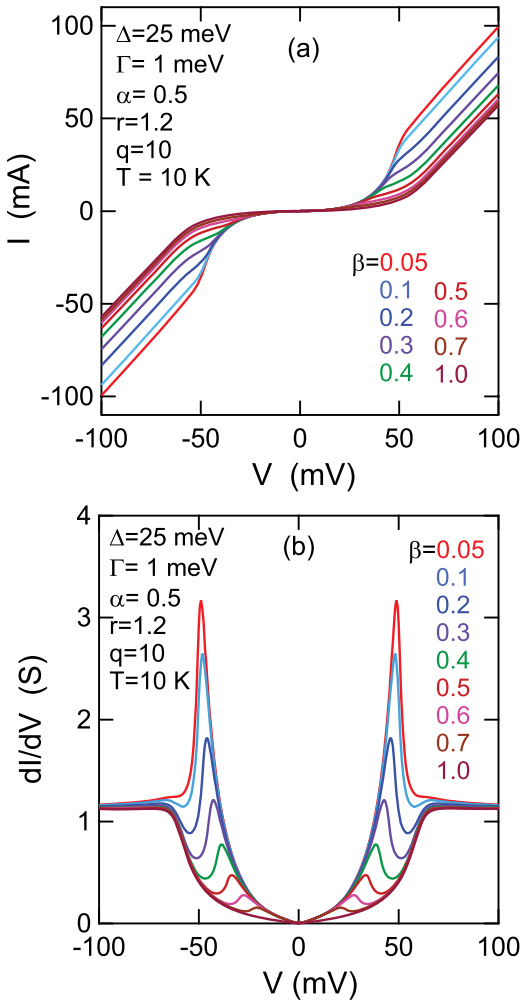

FIG. 6. (Color online) Calculated (a) I-V and (b) dI/dV-V curves for a set of parameters with values indicated in the figure and $\beta = \theta_0/(\pi/4)$ based on the present model, in which the contribution of the angular range in the d-wave order parameter is limited.

a parameter. It is readily seen that as the doping decreases (θ_0 increases, β increases); that is, as the length of the Fermi arc is reduced, the superconducting gap structure gradually diminishes and finally disappears by changing into a simple semiconducting gap structure. This behavior associated with doping is in good qualitative agreement with the experimental results.

The change brought about by doping is more clearly seen in the dI/dV-V characteristics in Fig. 6(b). As the doping decreases (β increases), the superconducting peak height decreases and shifts to lower energies. (This is because we set Δ_0 constant and did not take into account its doping dependence. Δ_0 actually increases with decreasing p.) Accompanying this change, a dip and hump structure shows up and, when β exceeds 0.3, the hump structure dominates the whole tunneling structure, which nearly corresponds to Figs. 4(a) and 4(b). There remain some discrepancies between the numerical results and the experimental results in the details of the characteristics, such as the shape of the hump structure. However, the qualitative agreement between Figs. 4 and 6 is sufficient to envisage this strongly **k**-dependent order parameter as a model to interpret the tunneling spectra and its evolution with doping in the Bi-2212 system. The numerical results are consistent with the significant doping dependence of J_c.

In the scanning tunneling spectroscopy (STS) measurements,[24,35,38] the tunneling occurs between the normal metal and a BSCCO crystal in the c axis direction. In this case, the tunneling spectra reflect the averaged quasiparticle DOS; that is, they exhibit both the superconducting peak and the semiconducting peak. By assuming a simple DOS for the semiconducting gap with the d-wave symmetry, such tunneling spectra can be calculated numerically.[39] The result is qualitatively consistent with the experimental results,[38,40] in which a coherence peak shifts toward higher energies and a pronounced pseudogap evolves with decreasing doping. The numerical result also gives a small cusp at a lower energy, which is also seen in the present experimental results.

C. Doping dependence of superfluid density

Since the IJJs are crystal structure itself, the IJJ characteristics represent the bulk properties of the Bi-2212 system. In this sense, the estimation of J_c through the IJJ provides a means to evaluate the magnitude of the superfluid density as is explained in the following.

The superfluid density ρ_s and its doping dependence in HTSCs have been estimated experimentally by several methods. These methods include measurements of μSR,[7,8,41] ac susceptibility,[42] lower critical field,[43] kinetic inductance,[44–46] surface impedance,[47] electron spin resonance (ESR),[48] and electronic specific heat.[49,50] The optical plasma frequency ω_p was also used to estimate ρ_s based on the common analytical expression between ω_p and the London penetration depth λ_L.[51] These methods are essentially based on the London model and provide relatively good estimates at least when the doping level is near the optimum or higher. The present method utilizing the IJJs can be regarded as another method to probe into the behavior of ρ_s in HTSCs, although the number of materials to which this method can be applied is limited.

In the Lawrence-Doniach (LD) model,[51,52] in the framework of which a stack of IJJs is reasonably represented, J_c is proportional to λ_c as described by

$$J_c = \hbar c^2/\left(8\pi d e \lambda_c^2\right), \tag{10}$$

where λ_c is the penetration depth when the magnetic field is in the ab plane and d is the separation of adjacent layers. It was shown that the anisotropy of $(\lambda_c/\lambda_{ab})^2$ is nearly equal to ρ_c/ρ_{ab}, where λ_{ab} is the magnetic penetration depth with the magnetic field along the c axis and ρ_{ab} is the resistivity in the ab plane.[53–56] Therefore, it is reasonable to think that J_c of IJJs reflects the superfluid density ρ_s in the Bi-2212 system. This implies that ρ_s changes as significantly as the experimental J_c, which decreases almost exponentially when p decreases from $p = 0.20$ to 0.09.

The doping dependence of ρ_s in HTSCs has been measured for $YBa_2Cu_3O_{7-y}$ (YBCO),[45,47,48,50] $La_{2-x}Sr_xCuO_4$ (LSCO),[44,49,50] and Bi-2212 systems.[50] The measurements of ρ_s in the underdoped region is sparse. This is mainly due to the difficulty in these measurements for underdoped specimens. For example, the μSR measurement is usually accompanied by difficulties due to contamination from the λ_c component or from magnetic moments which arise increasingly at underdoping levels, or from increasing degradation of flux line lattices at underdoping levels.[57] The method employing the electronic specific heat becomes much more difficult because the fraction of a change in the electronic specific heat decreases significantly at low doping levels and its separation from the background of the lattice specific heat becomes extremely difficult. Therefore, the method of measuring the kinetic inductance or the lower critical field was employed in the measurement of the doping dependence of ρ_s down to $p \sim 0.05$.[45,47]

In YBCO, ρ_s changes by a factor of $\sim$300 when p decreases from 0.2 to 0.054. In the case of LSCO, it was reported that ρ_s changes by a factor of 6.5 when p decreases from 0.24 to 0.07 based on the ac susceptibility and μSR measurements.[49] Compared with these results, ρ_s for the Bi-2212 system in the present study based on the LD model changes by a factor of 54 when p decreases from 0.2 to 0.09.[45] We compare the present result with that of YBCO. Then, it turns out that ρ_s for the Bi-2212 system in the present study decreases by a factor of 12 when p decreases from 0.16 to 0.09 at a much faster rate by a factor of 3 to 4 than in YBCO, where ρ_s decreases by a factor of $\sim$3.5 when p decreases from 0.16 to 0.09.[45] As for the reason for this rapid decrease in ρ_s, it should be first pointed out that the Fermi arcs exist in the underdoped Bi-2212 system, and the combination of the Fermi arcs and the d-wave superconducting order parameter causes the rapid decrease in ρ_s by a factor of more than 10. Although this value basically explains the significant decrease of ρ_s, it also implies that such a mechanism by itself may not be sufficient to explain the whole behavior of doping-dependent ρ_s. It is worth mentioning that the c-axis tunneling is **k** dependent and is the largest at $(\pi,0)$ and decreases toward the line node (π,π), where the tunneling probability becomes null.[58] If we further combine this mechanism with the d-wave and Fermi arc model, the significant decrease in J_c in Fig. 5(a) is quite explicable in terms of the present model.

Finally, an inhomogeneous $\Delta(\mathbf{r})$ in real space should be addressed. The STS results on the gap magnitude map[24,40,59] indicate that there are domains of various gap magnitudes. In the underdoped samples, a large proportion of domains are characterized by a broad peak centered at greater than 50 meV, which corresponds to the pseudogap. The domains of a sharp peak centered at less than 40 meV are sparse. These domains probably corresponds to the superconducting gap. The ratio of these two domains is approximately 0.05 to 0.1.[24] This value appears to be consistent the result in Fig. 5. However, if we consider extending the range of the superfluid, the size of superconducting domains, which ranges from 2 to 5 nm, is too small. Therefore, it is rather difficult to interpret the Δ maps as the distribution of Δ itself in real space. In the case of $\mathbf{k}$-dependent $\Delta(\mathbf{k})$, the tunneling probability varies from point to point unless the measurement point is commensurate. This implies that the superfluid density is homogeneous in real space, but the Δ map appears mosaic in real space. This argument is partly related with the Fourier transform of the real-space map, where an ordered pattern was observed in $\mathbf{k}$ space.[60]

When the doping level is reduced, the length of the Fermi arc decreases; namely, the range of $\mathbf{k}$ vectors for itinerant carriers is significantly reduced. In this situation, carriers are subject to the influence of crystalline imperfections and disorders, which can lead to local extinction of superconductivity. This is probable in underdoped Bi-2212, in which crystal imperfections are caused by atomic substitution. This gives rise to inhomogeneity in real space as a secondary effect.

V. CONCLUSIONS

We measured the interlayer tunneling spectra of the IJJs in the Bi-2212 system and found that the superconducting coherence peak evolves significantly as the doping level increases. Associated with the evolution of the superconducting peak, the pseudogap structure, which is prominent at low doping levels, gradually diminishes and almost disappears at overdoped levels. It is also found that J_c decreases by almost two orders of magnitude when the doping level was decreased from $p = 0.20$ to 0.09. This implies that the superfluid density is significantly reduced by nearly the same amount as the doping level is reduced. In order to interpret these behaviors, we have proposed a model, in which the superconducting order parameter is inhomogeneous in $\mathbf{k}$ space. This inhomogeneity is due to the Fermi arcs in the underdoped region when they are combined with the d-wave superconducting order parameter. This model explains qualitatively the significant decrease in the superfluid density. Based on this phenomenological model, the quasiparticle current-voltage characteristics are numerically calculated, giving a qualitatively good agreement.

*suzuki@kuee.kyoto-u.ac.jp

[1] D. A. Bonn, Nat. Phys. **2**, 159 (2006).
[2] C. Jaudet, D. Vignolles, A. Audouard, J. Levallois, D. LeBoeuf, N. Doiron-Leyraud, B. Vignolle, M. Nardone, A. Zitouni, R. Liang, D. A. Bonn, W. N. Hardy, L. Taillefer, and C. Proust, Phys. Rev. Lett. **100**, 187005 (2008).
[3] N. Doiron-Leyraud, C. Proust, D. LeBoeuf, J. Levallois, J. B. Bonnemasion, R. Liang, D. A. Bonn, W. N. Hardy, and L. Taillefer, Nature (London) **447**, 565 (2007).
[4] M. R. Norman, H. Ding, M. Randeria, J. C. Campuzano, T. Yokoya, T. Takahashi, T. Takeuchi, T. Mochiku, K. Kadowaki, P. Guptasarma, and D. G. Hinks, Nature (London) **392**, 157 (1998).
[5] T. Timusk and B. Statt, Rep. Prog. Phys. **62**, 61 (1999).
[6] C. C. Tsuei and J. R. Kirtley, Rev. Mod. Phys. **72**, 969 (2000).
[7] Y. J. Uemura *et al.*, Phys. Rev. Lett. **62**, 2317 (1989).
[8] Y. J. Uemura, L. P. Le, G. M. Luke, B. J. Sternlieb, W. D. Wu, J. H. Brewer, T. M. Riseman, C. L. Seaman, M. B. Maple, M. Ishikawa, D. G. Hinks, J. D. Jorgensen, G. Saito, and H. Yamochi, Phys. Rev. Lett. **66**, 2665 (1991).
[9] V. Ambegaokar and A. Baratoff, Phys. Rev. Lett. **10**, 486 (1963).
[10] R. Kleiner, F. Steinmeyer, G. Kunkel, and P. Müller, Phys. Rev. Lett. **68**, 2394 (1992).
[11] R. Kleiner and P. Müller, Phys. Rev. B **49**, 1327 (1994).
[12] T. Watanabe, T. Fujii, and A. Matsuda, Phys. Rev. Lett. **79**, 2113 (1997).
[13] J. L. Tallon, C. Bernhard, H. Shaked, R. L. Hitterman, and J. D. Jorgensen, Phys. Rev. B **51**, 12911 (1995).
[14] The value of $T_c^{max} = 89$ K is used for Bi-2212 crystals with [Bi] : [Sr] = 2.1 : 1.9 and 82.7 K for crystals with [Bi] : [Sr] = 2.2 : 1.8.[15]
[15] H. Eisaki, N. Kaneko, D. L. Feng, A. Damascelli, P. K. Mang, K. M. Shen, Z. X. Shen, and M. Greven, Phys. Rev. B **69**, 064512 (2004).
[16] M. Suzuki, T. Watanabe, and A. Matsuda, Phys. Rev. Lett. **82**, 5361 (1999).
[17] M. Suzuki, T. Watanabe, and A. Matsuda, IEEE Trans. Appl. Supercond. **9**, 4507 (1999).
[18] K. Anagawa, Y. Yamada, T. Shibauchi, M. Suzuki, and T. Watanabe, Appl. Phys. Lett. **83**, 2381 (2003).
[19] T. Hamatani, K. Anagawa, T. Watanabe, and M. Suzuki, Physica C **390**, 89 (2003).
[20] M. Suzuki, Y. Yamada, E. Tajitsu, and S. Kojima, IEEE Trans. Appl. Supercond. **17**, 594 (2007).
[21] The contact resistance R_{cont} was subtracted using an empirical formula $R_{cont} = a\exp(-b/T) + c/(T + d) + e$, where a–e are the fitting parameters. An example of a ρ_c-T curve before and after subtraction is seen in Ref. 61.
[22] Y. Yamada, K. Anagawa, T. Shibauchi, T. Fujii, T. Watanabe, A. Matsuda, and M. Suzuki, Phys. Rev. B **68**, 054533 (2003).
[23] A. Matsuda, S. Sugita, and T. Watanabe, Phys. Rev. B **60**, 1377 (1999).
[24] J. W. Alldredge, J. Lee, K. McElroy, M. Wang, K. Fujita, C. Taylor, H. Eisaki, S. Uchida, P. J. Hirschfeld, and J. C. Davis, Nat. Phys. **4**, 319 (2008).
[25] M. R. Norman, A. Kanigel, M. Randeria, U. Chatterjee, and J. C. Campuzano, Phys. Rev. B **76**, 174501 (2007).

[26] S. P. Zhao, X. B. Zhu, and H. Tang, Eur. Phys. J. B **71**, 195 (2009).
[27] W. S. Lee, I. M. Vishik, K. Tanaka, D. H. Lu, T. Sasagawa, N. Nagaosa, T. P. Devereaux, Z. Hussain, and Z. X. Shen, Nature (London) **450**, 81 (2007).
[28] K. Tanaka, W. S. Lee, D. H. Lu, A. Fujimori, T. Fujii, Risdiana, I. Terasaki, D. J. Scalapino, T. P. Devereaux, Z. Hussain, and Z.-X. Shen, Science **314**, 1920 (2006).
[29] A. Kanigel, M. R. Norman, M. Randeria, U. Chatterjee, S. Souma, A. Kaminski, H. M. Fretwell, S. Rosenkranz, M. Shi, T. Sato, T. Takahashi, Z. Z. Li, H. Raffy, K. Kadowaki, D. Hinks, L. Ozyuzer, and J. C. Campuzano, Nat. Phys. **2**, 447 (2006).
[30] J. Mannhart and H. Hilgenkamp, Mater. Sci. Eng., B **56**, 77 (1998).
[31] H. Hilgenkamp and J. Mannhart, Appl. Phys. Lett. **73**, 265 (1998).
[32] G. Hammerl, A. Schmehl, R. R. Schulz, B. Goetz, H. Bielefeldt, C. W. Schnekler, H. Hilgenkamp, and J. Mannhart, Nature (London) **407**, 162 (2000).
[33] S. Graser, P. J. Hirschfeld, T. Kopp, R. Gutser, B. M. Andersen, and J. Mannhart, Nat. Phys. **6**, 609 (2010).
[34] H. Ding, T. Yokoya, J. C. Campuzano, T. Takahashi, M. Randeria, M. R. Norman, T. Mochiku, K. Kadowaki, and J. Giapintzakis, Nature (London) **382**, 51 (1996).
[35] A. Pushp, C. V. Parker, A. N. Pasupathy, K. K. Gomes, S. Ono, J. Wen, Z. Xu, G. Gu, and A. Yazdani, Science **324**, 1689 (2009).
[36] B. Mitrović and L. A. Rozema, J. Phys.: Condens. Matter **20**, 015215 (2008).
[37] L. Ozyuzer, J. F. Zasadzinski, C. Kendziora, and K. E. Gray, Phys. Rev. B **61**, 3629 (2000).
[38] K. McElroy, D. H. Lee, J. E. Hoffman, K. M. Lang, J. Lee, E. W. Hudson, H. Eisaki, S. Uchida, and J. C. Davis, Phys. Rev. Lett. **94**, 197005 (2005).
[39] M. Suzuki, T. Hamatani, K. Anagawa, and T. Watanabe, in Proc. 26th International Conf. Low Temp. Phys., Beijing (2011) (to be published in J. Phys. Conf. Ser.).
[40] T. Machida, T. Kato, H. Nakamura, M. Fujimoto, T. Mochiku, S. Ooi, A. D. Thakur, H. Sakata, and K. Hirata, Phys. Rev. B **82**, 180507 (2010).
[41] E. H. Brandt, Phys. Rev. B **37**, 2349 (1988).
[42] J. R. Cooper, L. Forró, and B. Keszei, Nature (London) **343**, 444 (1990).
[43] R. Liang, D. A. Bonn, W. N. Hardy, and D. Broun, Phys. Rev. Lett. **94**, 117001 (2005).
[44] A. Rüfenacht, J. P. Locquet, J. Fompeyrine, D. Caimi, and P. Martinoli, Phys. Rev. Lett. **96**, 227002 (2006).
[45] I. Hetel, T. R. Lemberger, and M. Randeria, Nat. Phys. **3**, 700 (2007).
[46] Y. Zuev, M. S. Kim, and T. R. Lemberger, Phys. Rev. Lett. **95**, 137002 (2005).
[47] D. M. Broun, W. A. Huttema, P. J. Turner, S. Özcan, B. Morgan, R. Liang, W. N. Hardy, and D. A. Bonn, Phys. Rev. Lett. **99**, 237003 (2007).
[48] T. Pereg-Barnea, P. J. Turner, R. Harris, G. K. Mullins, J. S. Bobowski, M. Raudsepp, R. Liang, D. A. Bonn, and W. N. Hardy, Phys. Rev. B **69**, 184513 (2004).
[49] C. Panagopoulos, B. D. Rainford, J. R. Cooper, W. Lo, J. L. Tallon, J. W. Loram, J. Betouras, Y. S. Wang, and C. W. Chu, Phys. Rev. B **60**, 14617 (1999).
[50] J. L. Tallon, J. W. Loram, J. R. Cooper, C. Panagopoulos, and C. Bernhard, Phys. Rev. B **68**, 180501 (2003).
[51] C. C. Homes, S. V. Dordevic, M. Strogin, D. A. Bonn, R. Liang, W. N. Hardy, S. Komiya, Y. Ando, G. Yu, N. Kaneko, X. Zhao, M. Greven, D. N. Basov, and T. Timusk, Nature (London) **430**, 539 (2004).
[52] W. E. Lawrence and S. Doniach, in *Proceedings of the Conference on Low Temperature Physics, Kyoto* (Keigaku, Tokyo, 1971), pp. 361–362.
[53] T. Shibauchi, H. Kitano, K. Uchinokura, A. Maeda, T. Kimura, and K. Kishio, Phys. Rev. Lett. **72**, 2263 (1994).
[54] C. Panagopoulos, J. R. Cooper, N. Athanassopoulou, and J. Chrosch, Phys. Rev. B **54**, R12721 (1996).
[55] T. Jacobs, S. Sridhar, Q. Li, G. D. Gu, and N. Koshizuka, Phys. Rev. Lett. **75**, 4516 (1995).
[56] C. Panagopoulos, J. R. Cooper, T. Xiang, G. B. Peacock, I. Gameson, and P. P. Edwards, Phys. Rev. Lett. **79**, 2320 (1997).
[57] C. Niedermayer, C. Bernhard, T. Blasius, A. Golnik, A. Moodenbaugh, and J. I. Budnick, Phys. Rev. Lett. **80**, 3843 (1998).
[58] L. B. Ioffe and A. J. Millis, Phys. Rev. B **58**, 11631 (1998).
[59] K. K. Gomes, A. N. Pasupathy, A. Pushp, S. Ono, Y. Ando, and A. Yazdani, Nature (London) **447**, 569 (2007).
[60] K. McElroy, R. W. Simmonds, J. E. Hoffman, D. H. Lee, J. Orenstein, H. Eisaki, S. Uchida, and J. C. Davis, Nature (London) **422**, 592 (2003).
[61] M. Suzuki, T. Hamatani, Y. Yamada, K. Anagawa, and T. Watanabe, J. Phys. Conf. Ser. **150**, 052252 (2009).